TRANSPORT COEFFICIENTS IN SOME STOCHASTIC MODELS OF THE REVISED ENSKOG EQUATION

JACEK POLEWCZAK AND GEORGE STELL

Abstract. A stochastic model of the revised Enskog equation is considered. A choice of the smearing function suggested by the work of Leegwater ([1]) is used to apply the model to the repulsive part of the Lennard-Jones potential and the inverse-power soft-sphere potential. The virial coefficients obtained from the equilibrium properties of the models are in excellent agreement with the known exact coefficients for these models. The transport coefficients for the repulsive Lennard-Jones (RLP) model are also computed and appear to be of comparable accuracy to the Enskog-theory coefficients applied directly to a hard-sphere system, although exact results for the RLP with which to make an extensive comparison are not yet available. The pressure and the transport coefficients obtained from the model (shear viscosity, thermal conductivity, and self-diffusion) are compared with the pressure and the corresponding transport coefficients predicted by the Enskog and square-well kinetic theories.

1. Introduction

One of the important goals of any kinetic theory is its capability to compute transport coefficients of a fluid. The kinetic theory based on the Boltzmann equation, valid in the regime of close–to–zero densities (dilute–gas regime), produces the transport coefficients of an ideal fluid. For moderately dense, hard–sphere gases, the kinetic theory based on the standard or revised Enskog equations ([2], [3], [4]) describes, on the hydrodynamical level, a non–ideal fluid with transport coefficients having a nonvanishing bulk viscosity. In order to account for more realistic potentials (other than hard–core potentials) several extensions of the revised Enskog equation have been proposed. Since smooth potentials can be approximated by a sequence of step functions, the square-well potential ϕ^{SW} can be considered as the lowest-order approximation of this type. For $\epsilon > 0,\ 0 < a < R$, and

$$\phi^{SW}(r) = \begin{cases} \infty, & \text{for } r \le a, \\ -\epsilon, & \text{for } a < r < R, \\ 0 & \text{for } r \ge R. \end{cases} \tag{1.1}$$

the authors in [5], [6], [7], [8], [9], and [10] have developed new models of kinetic theories. Recent ones are based on the maximization of the fine–grained entropy, subject to appropriate constraints, which yields what has come to be called kinetic variational theory (KVT). Use of a set of increasingly stringent constraints which are a subset of the exact constraints in the problem seem to provide

Key words and phrases. Kinetic theory of gases, Enskog theory, hard spheres systems, Lennard-Jones potential, transport coefficients.

We fondly dedicate this work to Bob Dorfman, who has lent G. S. a sympathetic ear to various notions of disequilibrium for the last four decades.

The authors gratefully acknowledge the support of this work by the Division of Chemical Sciences, Office of Basic Energy Sciences, Office of Energy Research, U.S. Department of Energy.

increasingly accurate quantitative assessments of transport coefficients and related macroscopic quantities. In particular, the version that is based upon a local energy–density constraint (called by the authors KVTIII, because it is generated by the third in the sequence of constraints mentioned above) has been investigated in detail and the transport coefficients obtained from the KVTIII are in good agreement with experimental data and computer simulation results for moderately dense fluids.

Although this progress has been encouraging, there have been no fully satisfactory extensions of these theories to more realistic pair potentials that have soft rather than hard cores and smoothly varying attractive tails with no discontinuities. Karkheck, Stell and Xu [11] applied KVTIII to a truncated Lennard-Jones (LJ) potential to obtain formal KVTIII expressions for the full LJ limit, in which the point of truncation goes to infinity, but the temporal approach to equilibrium in KVTIII has certain pathological features in this limit. Although the KVTIII transport coefficients themselves are robust and generally useful for a moderately dense LJ fluid, the KVTIII does a relatively poor job in capturing the quantitative behavior of the diffusion coefficient as a function of temperature. Subsequently, in his thesis, J. A. Leegwater [1] considered a new approach to obtaining the self-diffusion coefficient of an LJ system from Enskog-theory expressions into which a weighing factor W(r) is introduced to accommodate the soft LJ potential. The resulting expression has the form

$$D = \frac{3}{8n}\frac{1}{\left(\int_0^\infty W(r)y(r)\,dr\right)}\left(\frac{k_BT}{\pi m}\right)^{1/2}, \tag{1.2}$$

where $y(r) = \exp\left[\beta\phi^{LJ}(r)\right] g_2^{LJ}(r)$ is the cavity function, ϕ^{LJ} is the Lennard-Jones potential,

$$\phi^{LJ}(r) = 4\epsilon\left[\left(\frac{d}{r}\right)^{12} - \left(\frac{d}{r}\right)^{6}\right], \tag{1.3}$$

$g_2^{LJ}(r)$ is the equilibrium radial correlation function of the Lennard-Jones system, and $W(r)$ is a certain weighting function that was obtained by solving approximately the two particle equations of motion. Because the LJ y(r) is very well approximated by a hard-sphere y(r) for a suitably chosen hard-sphere diameter, one can simply use a hard-sphere y(r) in (1.2). Leegwater's idea was to generalize the expression for the Enskog value of the self-diffusion coefficient,

$$D^{Enskog} = \frac{3}{8n}\frac{1}{a^2 g_2^{HS}(a^+)}\left(\frac{k_BT}{\pi m}\right)^{1/2}, \tag{1.4}$$

(here $g_2^{HS}(a^+)$ is the contact value of hard-spheres' radial correlation function) to continuous potentials, by an *ad hoc* insertion into (1.4) the factor g_2^{LJ}, weighted by the function $W(r)$. Furthermore, since Leegwater's $W(r)$ satisfies the normalization condition

$$\int_0^\infty \frac{W(r)}{r^2}\,dr = 1, \tag{1.5}$$

the approximation (1.2) reduces to (1.4) in the hard-sphere limit.

In this work we provide new arguments for validity of the approximate formula (1.2) for the self–diffusion coefficient. In addition, we derive the corresponding formulas for other transport coefficients, not considered by Leegwater. We start by introducing a class of the kinetic equations that have built into their structure the weighting function $W(a)$. Then, by linearizing the equation around absolute equilibrium, we derive the formulas for the transport coefficients. The resulting expressions yield formula (1.2) for the self-diffusion coefficient (with $y(r)$ taken to be the hard-sphere $y(r)$) and corresponding formulas for shear viscosity and thermal conductivity. Finally, we provide numerical comparison of the pressure and the transport coefficients obtained from our model with the corresponding values of pressure and transport coefficients obtained from the Enskog and square-well kinetic theories.

2. The kinetic equation

We start with the revised Enskog equation and perturb it by smearing effects in the collisional processes. This is done by introducing varying diameters of hard spheres. Particles' diameters vary according to a certain (possibly time dependent) probability density $P(t,a)$ that may also depend on the velocity moments (i.e., macroscopic quantities like density, velocity, and temperature) of the one-particle distribution function $f(t,x,v)$. The kinetic equation has the form:

$$\frac{\partial f}{\partial t} + v\frac{\partial f}{\partial x} = E_{stoch}(f) \equiv E^{+}_{stoch}(f) - E^{-}_{stoch}(f), \tag{2.1}$$

with

$$E^{+}_{stoch}(f) = \iiint\limits_{[\alpha_1,\alpha_2]\times\mathbb{R}^3\times\mathbb{S}^2_+} f(t,x,v')f(t,x-a\epsilon,w')a^2P(t,a)g_2(x,x-a^+\epsilon\,|\,n(t,\cdot))\langle\epsilon,v-w\rangle\,d\epsilon dw da, \tag{2.2}$$

$$E^{-}_{stoch}(f) = \iiint\limits_{[\alpha_1,\alpha_2]\times\mathbb{R}^3\times\mathbb{S}^2_+} f(t,x,v)f(t,x+a\epsilon,w)a^2P(t,a)g_2(x,x+a^+\epsilon\,|\,n(t,\cdot))\langle\epsilon,v-w\rangle\,d\epsilon dw da. \tag{2.3}$$

Here, $\langle\cdot,\cdot\rangle$ is the inner product in $\mathbb{R}^3$, $\epsilon \in \mathbb{S}^2_+ = \{\epsilon\in\mathbb{R}^3 : |\epsilon| = 1, \langle\epsilon, v-w\rangle \geq 0\}$, θ is the angle between ϵ and $v-w$ (i.e., $|v-w|\cos\theta = \langle\epsilon,v-w\rangle$), $0 \leq \alpha_1 < \alpha_2$, and

$$v' = v - \epsilon\langle\epsilon, v-w\rangle, \qquad w' = w + \epsilon\langle\epsilon,v-w\rangle. \tag{2.4}$$

Furthermore, g_2 is the pair correlation function of the hard-sphere system at non-uniform equilibrium, with the local density $n(t,r)$. The notation $g_2(x_1,x_2\,|\,n(t,\cdot))$ indicates that g_2 is a functional of n. The form of $g_2(x_1,x_2\,|\,n(t,\cdot))$ is given by the following Mayer cluster expansion:

$$\begin{aligned} &g_2(x_1,x_2\,|\,n) = \exp(-\beta\phi^{HS}(|x_1-x_2|))\times \\ &\Big\{1+\int V(12\,|\,3)n(t,x_3)\,dx_3 + \frac{1}{2}\int\int V(12\,|\,34)n(t,x_3)\,n(t,x_4)\,dx_3dx_4 + \cdots + \\ &\frac{1}{(k-2)!}\int dx_3\,\cdots\int dx_k\,n(3)\,\cdots\,n(k)\,V(12\,|\,3\ldots k) + \cdots\Big\}, \end{aligned} \tag{2.5}$$

where $n(k) = n(t,x_k)$, $\beta = 1/k_BT$, $V(12\,|\,3\ldots k)$ is the sum of all graphs of k labeled points which are biconnected when the Mayer factor $f_{ij} = \exp(-\beta\phi^{HS}(|x_i-x_j|)) - 1$ is added. Here, ϕ^{HS} is the hard-sphere potential

$$\phi^{HS}(r) = \begin{cases} +\infty, & \text{if } r\leq\sigma; \\ 0, & \text{if } r>\sigma, \end{cases} \tag{2.6}$$

Remark 1. In this work, we assume that the series in (2.5) is pointwise convergent, at least for small densities n. It is known that in the homogeneous case ($n = const$), the series in (2.5) is convergent for sufficiently small densities n (see, for example, [16]).

The function P appearing in (2.2)-(2.3) is a nonnegative probability density, which introduces a *smearing–type* effect in the collision process. Collisions are smeared in the domain (determined by the interval $[\alpha_1, \alpha_2]$, with $\alpha_1 > 0$) around the points of impact. In the case $P(t, a) = \delta(a - \sigma)$ for all t and $\sigma \in [\alpha_1, \alpha_2]$, with $\sigma > 0$, equation (1.2) reduces to the revised Enskog equation for hard spheres with the diameter σ.

Similar models to (2.1) had been known for the Boltzmann equation [12]. From the mathematical point of view, the authors in [13] (see also references in [14]) utilized similar searing-type effects and were able to pass to the Euler level from a stochastic BBGKY-hierachy equations, while the authors in [15] proved the convergence to absolute equilibrium for the stochastic (Povzner-like) Boltzmann equation.

The equation (2.1) introduces an additional integration into the collisional operator E_{stoch} given by (2.2)–(2.3). Combined with the two–dimensional integration with respect to $\langle \epsilon, v - w \rangle$, the integration with respect to a in formulas (2.2)–(2.3) amounts to a three–dimensional integration in the spatial variable x of the distribution function f. This fact had played an important role in proving various existence theorems for the corresponding equations (see, for example, [12],[13], [14], and [15]) While theoretical advantages of the above model are important and had been considered in the just quoted reference, in this work, we will be concerned with providing examples of viable prescriptions for the weight function $P(t, a)$.

Equation (2.1) exhibits several properties that are analogous to the corresponding properties of the revised Enskog equation. First, for ψ measurable on $\Omega \times \mathbb{R}^3$ and $f \in C_0(\Omega \times \mathbb{R}^3)$, we have

$$\begin{aligned}
&\iint\limits_{\Omega\times\mathbb{R}^3} \psi(x, v) E_{stoch}(f)\, dvdx = \\
&\qquad \frac{1}{2} \int\limits_{\Omega\times\mathbb{R}^3\times[\alpha_1,\alpha_2]\times\mathbb{R}^3\times\mathbb{S}^2_+} \!\!\!\cdots\!\!\! \int \Big[\psi(x, v') + \psi(x + a\epsilon, w') - \psi(x, v) - \psi(x + a\epsilon, w)\Big] \times \\
&\qquad f(t, x, v) f(t, x + a\epsilon, w) a^2 P(t, a) g_2(x, x + a^+\epsilon \,|\, n(t, \cdot)) \langle \epsilon, v - w \rangle \, d\epsilon dw da dv dx.
\end{aligned} \tag{2.7}$$

For $\psi = 1$, $\psi = v$, and $\psi = v^2$, the left hand side of identity (2.7) is identically zero; this property corresponds to conservation of the mass, momentum, and energy. $\Omega \subset \mathbb{R}^3$ denotes a spatial domain, which (for simplifications only) is either equal to $\mathbb{R}^3$ or $\mathbb{R}^3/\mathbb{Z}^3$, a 3-dimensional torus. The latter choice corresponds to case of the periodic boundary conditions on $[0, L]^3$ and some $L > 0$.

Another important property of the model (2.1)-(2.3) is existence of a Liapunov functional. As in [17] one shows that, for nonnegative solutions f of equation (2.1), $\Gamma_{stoch}(t)$ defined by

$$\Gamma_{stoch}(t) = H_{ideal}(f)(t) + H_{corr}(f)(t) = \iint\limits_{\Omega\times\mathbb{R}^3} f(t, x, v) \log f(t, x, v)\, dvdx - \int_0^t I(s)\, ds \tag{2.8}$$

with

$$\begin{aligned}
I(t) = \frac{1}{2} \int\limits_{\Omega\times\mathbb{R}^3\times[\alpha_1,\alpha_2]\times\mathbb{R}^3\times\mathbb{S}^2_+} \!\!\!\cdots\!\!\! \int &\Big[f(t, x, v') f(t, x + a\epsilon, w') - f(t, x, v) f(t, x + a\epsilon, w)\Big] \times \\
&a^2 P(t, a) g_2(x, x + a\epsilon \,|\, n(t, \cdot)) \langle \epsilon, v - w \rangle \, d\epsilon dw da dv dx,
\end{aligned} \tag{2.9}$$

has the property

$$\frac{d\Gamma_{stoch}}{dt} \leq 0. \tag{2.10}$$

The equality in (2.10) holds if and only if

$$f(t,r,v) = n(t,r)\big(\beta(t)m/2\pi\big)^{3/2}\exp\big(-\beta(t)m(v-u(t))^2/2\big), \tag{2.11}$$

where $u(t)$ is fluid velocity and $\beta(t) = 1/k_B T(t)$ with $T(t)$ fluid kinetic temperature. We observe that the form of f in (2.11) is identical to the one in the revised Enskog equation and, in addition, it is **independent** of the function $P(t,a)$ in the definition (2.8)–(2.9) of the functional $\Gamma_{stoch}(t)$. At the same time, as we will show in the next section, that the relation between macroscopic n and T (the equation of state), as well as the expressions for transport coefficients do depend on choices of $P(t,a)$.

As in the case of the revised Enskog equation, one can express the correlation part of the Liapunov functional, $H_{corr}(f)(t)$, in terms of the Mayer diagrams. Indeed, using very similar arguments as in [18], we obtain

Theorem 2.1. *For each nonnegative $P(t,a)$, the kinetic model (2.1)–(2.3) has an H–function*

$$H_{stoch}(t) = \iint_{\Omega\times\mathbb{R}^3} f(t,x,v)\log f(t,x,v)\,dvdr - \sum_{k=2}^{\infty}\frac{1}{k!}\int_{\alpha_1}^{\alpha_2} P(t,a)da\int_{\Omega} dx_1\cdots dx_k n(1)\ldots n(k)V_a(1\ldots k)$$
$$+\int_0^t\sum_{k=2}^{\infty}\frac{1}{k!}\int_{\alpha_1}^{\alpha_2}\frac{\partial P(s,a)}{\partial s}\int_{\Omega} dx_1\cdots dx_k n(1)\ldots n(k)V_a(1\ldots k)\,dads, \tag{2.12}$$

with $V_a(1\ldots k)$ the sum of all irreducible Mayer graphs that doubly connect k particles with the (fictitious) diameter a

We observe that when $P(a) = \delta(a-\sigma)$, with $0 < \sigma \in (\alpha_1,\alpha_2)$, $H_{stoch}(t)$ reduces itself to the H–function for the revised Enskog equation.

Remark 2. In the case when P depends also on the macroscopic quantities n, u, and/or T (moments of f), expression (2.12) for H_{stoch} is no longer true; however, a generalized form of (2.8)-(2.9) still holds. This topic will be pursued in our forthcoming paper.

3. The transport coefficients and the equation of state

In this section we provide explicit formulas for the transport coefficients and equation of state that correspond of the fluid which is described on the kinetic level by equation (2.1)–(2.3). One of the important and characteristic features of our model is the fact that the transport coefficients as well as the equation of state can be computed explicitly in terms of function $P(a)$.

As it is well known, there is no advantage in treating the original (nonlinear) equation as far as the computation of transport coefficients is concerned. What is, in fact, needed is the linearization of equation (2.1)–(2.3) around the absolute equilibrium, $n\omega$, with

$$\omega = (2\pi k_B T/m)^{-3/2}\exp\left(-\frac{mv^2}{2k_B T}\right), \tag{3.1}$$

and some perturbation calculus applied to the corresponding eigenvalue problem.

The linearized (around absolute maxwellian (3.1)) collision operator is the functional derivative, $(\partial E_{stoch}/\partial f)\,(n\omega)$, evaluated at $n\omega$, which acts as an operator on a given function $h(r,v)$. When one carefully defines E_{stoch} to be a map between some Banach spaces X and Y, then $(\partial E_{stoch}/\partial f)\,(n\omega)$ can be defined as the Fréchet derivative, $D_{n\omega}E_{stoch}$, that is a bounded linear operator from X into Y. For the purpose of evaluating transport coefficients alone we limit ourselves to formal expression of $D_{n\omega}E_{stoch}$. Below, $g_2(n,a^+)$ denotes the contact value (i.e., for x_1, x_2 with $|x_1 - x_2| = a^+$) of $g_2(x_1,x_2\,|\,n(\cdot))$ corresponding to a homogeneous (i.e. constant) density n. Also, for each $h(x,v)$, $n_h(x) \equiv \int_{R^3} h(x,v)\,dv$. We have

$$D_{n\omega}E_{stoch}h = C^1h + C^2h, \tag{3.2}$$

with

$$C^1h = n \iiint\limits_{[\alpha_1,\alpha_2]\times\mathbb{R}^3\times\mathbb{S}^2_+} \Big[h(x,v')\omega(w') + \omega(v')h(x-a\epsilon,w') - h(x,v)\omega(w) - \omega(v)h(x+a\epsilon,w)\Big]\times$$
$$a^2P(a)g_2(n,a^+)\langle\epsilon, v-w\rangle\, d\epsilon dw da, \tag{3.3}$$

and

$$C^2h = n^2 \iiint\limits_{[\alpha_1,\alpha_2]\times\mathbb{R}^3\times\mathbb{S}^2_+} \Big[D_ng_2(x,x-a\epsilon\,|\,n(\cdot))n_h - D_ng_2(x,x+a\epsilon\,|\,n(\cdot))n_h\Big]\times$$
$$\omega(v)\omega(w)a^2P(a)g_2(n,a^+)\langle\epsilon, v-w\rangle\, d\epsilon dw da, \tag{3.4}$$

where $D_ng_2(x,x\pm a\epsilon\,|\,n(\cdot))n_h$ are the functional (Fréchet) derivatives, evaluated at n, and acting on n_h. The first two terms of $D_ng_2(x,x\pm a\epsilon\,|\,n(\cdot))n_h$ are as follows:

$$D_ng_2(x_1,x_2\,|\,n(\cdot))n_h =$$
$$\Theta_{12}\left\{\int\limits_{\Omega} V(12\,|\,3)n_h(3)\,dx_3 + \frac{n}{2}\iint\limits_{\Omega\times\Omega} V(12\,|\,34)\,[n_h(3)+n_h(4)]\;dx_3dx_4 + \cdots\right\}, \tag{3.5}$$

where $\Theta_{12} = \Theta(|x_1 - x_2|)$ with Θ, the Heaviside function.

Next, we perform the Fourier transformation of $D_{n\omega}E_{stoch}h$ (denoted by $L_\xi h_\xi$), with $h_\xi(v) = \int \exp(-i\langle\xi,x\rangle)h(x,v)\,dx$, $i = \sqrt{-1}$, and $\xi = (\xi_1,0,0)$. Due to the fact that we are interested in the hydrodynamics modes, we keep only the terms up to the order $|\xi|^2$ in the Taylor expansion in $|\xi|$ of the function $L_\xi h_\xi$. The result is

$$L_\xi h_\xi = L^Bh_\xi + i\xi_1L^{(1)}h_\xi - (\xi_1)^2L^{(2)}h_\xi + O(|\xi_1|^3), \tag{3.6}$$

where

$$L^Bh_\xi = n \iiint\limits_{[\alpha_1,\alpha_2]\times\mathbb{R}^3\times\mathbb{S}^2_+} \Big[h_\xi(x,v')\omega(w') + \omega(v')h_\xi(x,w') - h_\xi(x,v)\omega(w) - \omega(v)h_\xi(x,w)\Big]\times$$
$$a^2P(a)g_2(n,a^+)\langle\epsilon, v-w\rangle\, d\epsilon dw da, \tag{3.7}$$

$$L^{(1)}h_\xi = n \iint\limits_{[\alpha_1,\alpha_2]\times\mathbb{R}^3\times\mathbb{S}^2_+} \Big[h_\xi(w')\omega(v') + \omega(w')h_\xi(v')\Big]\epsilon_1 a^3 P(a) g_2(n,a^+)\langle\epsilon, v-w\rangle\, d\epsilon dw da$$

$$+ n^2 \left(\int\limits_{\mathbb{R}^3} h_\xi(v_1)\, dv_1\right) \iiint\limits_{[\alpha_1,\alpha_2]\times\mathbb{R}^3\times\mathbb{S}^2_+} \omega(v)\omega(w)\epsilon_1 a^3 P(a)\frac{\partial g_2(n,a^+)}{\partial n}\langle\epsilon, v-w\rangle\, d\epsilon dw da, \quad (3.8)$$

and

$$L^{(2)}h_\xi = \frac{n}{2} \iiint\limits_{[\alpha_1,\alpha_2]\times\mathbb{R}^3\times\mathbb{S}^2_+} \Big[h_\xi(x,w')\omega(v') - \omega(v)h_\xi(x,w)\Big] a^4 P(a) g_2(n,a^+)\epsilon_1\langle\epsilon, v-w\rangle\, d\epsilon dw da. \quad (3.9)$$

Here, $\epsilon = (\epsilon_1, \epsilon_2, \epsilon_3)$ and $\frac{\partial g_2(n,a^+)}{\partial n}$ is equal to the right hand side of (3.5) evaluated at contact value (i.e., for $|x_1 - x_2| = a^+$) and with $n_h \equiv 1$.

Now, as in the case of the Enskog equation (see, [4], pp. 165-167), in order to compute transport coefficients we consider the following eigenvalue problem

$$\left[L^B + i\xi_1(L^{(1)} - v_1) - (\xi_1)^2 L^{(2)}\right]\phi = \lambda\phi, \quad (3.10)$$

where $v = (v_1, v_2, v_3)$ Using perturbation analysis up to the second order in ξ_1, we obtain for the shear viscosity,

$$\eta^{stoch} = -nm \lim_{\tau\to 0^+}\left\langle \phi_3 \,\middle|\, \left(L^{(1)} - v_1\right)\left(L^B - \tau\right)^{-1}\left(L^{(1)} - v_1\right) \,\middle|\, \phi_3\right\rangle + nm\left\langle \phi_3 \,\middle|\, L^{(2)} \,\middle|\, \phi_3\right\rangle, \quad (3.11)$$

and for the heat conductivity

$$\kappa^{stoch} =$$

$$- nmC_p \lim_{\tau\to 0^+}\left\langle \left(-\phi_1 + (3/2)^{1/2}\phi_5\right) \,\middle|\, \left(L^{(1)} - v_1\right)\left(L^B - \tau\right)^{-1}\left(L^{(1)} - v_1\right) \,\middle|\, \left(-\phi_1 + (3/2)^{1/2}\phi_5\right)\right\rangle$$

$$+ nm\left\langle \left(-\phi_1 + (3/2)^{1/2}\phi_5\right) \,\middle|\, L^{(2)} \,\middle|\, \left(-\phi_1 + (3/2)^{1/2}\phi_5\right)\right\rangle, \quad (3.12)$$

where $\langle g\,|\,h\rangle = \int_{\mathbb{R}^3} g^*(v)h(v)\omega^{-1}(v)\, dv$, with $*$ denoting the complex conjugate, C_p is the specific heat, and ϕ_i, for $i = 1, 2, 3, 4, 5$, are the normalized eigenfunctions corresponding to the eigenvalue $\lambda = 0$ of L^B:

$$\phi_1 = \omega \quad (3.13a)$$

$$\phi_i = \frac{v_i}{\sqrt{k_B T/m}}\omega, \qquad (i = 2, 3, 4), \quad (3.13b)$$

$$\phi_5 = \sqrt{\frac{2}{3}}\left(\frac{mv^2}{2k_B T} - \frac{3}{2}\right)\omega. \quad (3.13c)$$

It is important to observe that the operator L^B is precisely the linearized Boltzmann operator with the scattering kernel $B(\theta, |v - w|)$ given by

$$B(\theta, |v-w|) = \left(\int_{\alpha_1}^{\alpha_2} a^2 P(a) g_2(n,a^+)\, da\right)\langle\epsilon, v-w\rangle. \quad (3.14)$$

In the cases when the operators $L^{(1)}$ and $L^{(2)}$ approach zero (in a suitable sense), formulas (3.11)–(3.12) reduce to the corresponding transport coefficients given by the kinetic theory based on the

Boltzmann equation with the scattering kernel $B(\theta, |v-w|)$ given in (3.14). This is, for example, the case for $P(a) = \delta(a-\sigma)$, and after one takes the dilute–gas limit, i.e., when $n\sigma^3 \to 0$.

Finally, using computations similar to those in the case of the Enskog equation (e.g., [4], page 166-167), we obtain from (3.11)–(3.12)

$$\eta^{stoch} = \left(1 + \frac{2}{5}n\int_{\alpha_1}^{\alpha_2} b^E(a)P(a)g_2(n,a^+)\,da\right)^2 \eta^B + \frac{3}{5}\zeta^{stoch}, \tag{3.15}$$

for the shear viscosity, and

$$\kappa^{stoch} = \left(1 + \frac{3}{5}n\int_{\alpha_1}^{\alpha_2} b^E(a)P(a)g_2(n,a^+)\,da\right)^2 \kappa^B + C_v\zeta^{stoch}, \tag{3.16}$$

for the heat conductivity, where ζ^{stoch} is analogous to the bulk viscosity given by

$$\zeta^{stoch} = \frac{n^2\sqrt{mk_BT}}{\pi^{3/2}}\int_{\alpha_1}^{\alpha_2} \frac{(b^E(a))^2}{a^2}P(a)g_2(n,a^+)\,da, \tag{3.17}$$

with $b^E(a) = 2\pi a^3/3$ and C_v equal to the specific heat. The coefficients η^B and κ^B are equal to the hard–spheres Boltzmann shear viscosity and heat conductivity. They are given by

$$\eta^B = \lim_{\tau\to 0^+}\left\langle \phi_3 \middle| v_1\left(L^B-\tau\right)^{-1}v_1 \middle| \phi_3\right\rangle, \tag{3.18}$$

and

$$\kappa^B = \frac{2}{5}\lim_{\tau\to 0^+}\left\langle \left(-\phi_1 + (\frac{3}{2})^{1/2}\phi_5\right) \middle| v_1\left(L^B-\tau\right)^{-1}v_1 \middle| \left(-\phi_1 + (\frac{3}{2})^{1/2}\phi_5\right)\right\rangle, \tag{3.19}$$

where L^B (given in (3.7)) is the hard–spheres linearized Boltzmann operator, with the diameter σ equal to

$$\sigma = \left(\int_{\alpha_1}^{\alpha_2} a^2P(a)g_2(n,a^+)\,da\right)^{1/2}. \tag{3.20}$$

We observe again that when $P(a) = \delta(a-\sigma)$, with $\sigma > 0$, expressions (3.15)–(3.16) reduce to the Enskog equation formulas for the shear viscosity and the heat conductivity, respectively.

In analogous way, by considering instead, suitably modified, the Boltzmann–Lorentz equation one obtains that the corresponding self–diffusion coefficients is given by

$$D^{stoch} = \frac{3}{8n}\frac{1}{\left(\int_{\alpha_1}^{\alpha_2} a^2P(a)g_2(n,a^+)\,da\right)}\left(\frac{k_BT}{\pi m}\right)^{1/2}. \tag{3.21}$$

The similarity between (3.21) and Leegwater's formula (1.2) for self-diffusion coefficient is remarkable. In contrast to the heuristic approach of Leegwater, our formulas for the self-diffusion, as well as for the shear viscosity and thermal conductivity transport coefficients, are derived from the kinetic model (2.1) that has built-in conservation laws and trend to equilibrium. It is at this stage that we make a connection between Leegwater's formula (1.2) and our model through the following identification:

$$a^2P(a) \sim W(a). \tag{3.22}$$

We observe that this identification is consistent with the normalization condition for P, in our model,

$$\int_{\alpha_1}^{\alpha_2} P(a)\,da = 1, \tag{3.23}$$

and Leegwater's normalization condition (1.5). Normalization (3.23) guarantees that our model reduces itself to the revised Enskog equation in the hard-sphere limit, while the normalization (1.5) guarantees that approximation (1.2) satisfies the desired (Enskog) hard sphere limit.

What Leegwater's approach provides us is a sensible physical argument for a particular choice of P(a), through W(r), based upon two-particle dynamics associated with a particular soft potential, such as the RLJ or inverse-power potential, defined in (3.24). However, we note that we can not apply our stochastic-model approach directly to the full LJ potential, because our P(a) is a probability , which must be nonnegative, whereas Leegwater's W(a) (and hence the associated P(a), via (3.22)) is not a nonnegative function. This is because the LJ potential takes negative as well as positive values. Actually, Leegwater's derivation is more legitimately applicable to repulsive potentials in the first place, because of its neglect of bound states in considering two-particle dynamics in the presence of a fluid of like particles.

We consider two types of potentials: (1) the repulsive parts of the LJ potential (RLJ) and (2) the inverse-power potential (sometimes referred to as the point centers of repulsion-soft spheres potential or soft-sphere potential)

$$(1)\quad \phi^r(r) = \begin{cases} 4\epsilon\left[\left(\frac{d}{r}\right)^{12} - \left(\frac{d}{r}\right)^{6}\right] + \epsilon, & \text{for } r \leq 2^{\frac{1}{6}}d; \\ 0, & \text{for } r > 2^{\frac{1}{6}}d, \end{cases} \qquad (2)\quad \phi^s = \gamma\left(\frac{d}{r}\right)^m, \quad m \geq 6. \tag{3.24}$$

The potential $\phi^r(r)$ is always nonnegative and $\phi^r\left(2^{1/6}d\right) = 0$. Furthermore, it is well known that for $\gamma = 1$, $\phi^s \to \phi^{HS}$, as $n \to \infty$, where ϕ^{HS} is the hard-sphere potential (2.6) with the diameter d.

In order for us to treat the full LJ potential using our stochastic-model technique, we must use as a starting point the KVTIII expressions for the square-well potential and introduce into them a $P_1(a)$ to describe a distribution of hard-core diameters and a separate $P_2(a)$ to describe a distribution of square-well diameters, with $P_2(a)$ tailored to describe the shape of the LJ attractive bowl.

We end this section by providing an explicit formula for the equation of state of the fluid underlying the stochastic kinetic model (2.1)-(2.3). Arguing similarly as in the case of the Enskog equation (see again, [4]) one obtains

$$\frac{p}{nk_BT} = 1 + n\int_{\alpha_1}^{\alpha_2} b^E(a)P(a)g_2(n,a^+)\,da, \tag{3.25}$$

where $b^E(a) = 2\pi a^3/3$ and $g_2(n,a^+)$ is the radial correlation function (at uniform equilibrium) for the system of hard spheres with diameter a. As before, when $P(a) = \delta(a-\sigma)$, equation (3.25) reduces itself to the equation of state for hard-sphere system with diameter σ:

$$\frac{p}{nk_BT} = 1 + \left(\frac{2\pi\sigma^3}{3}\right) ng_2(n,\sigma^+). \tag{3.26}$$

4. Numerical computations and comparisons of pressure and transport coefficients

4.1. **Comparisons of the virial coefficients.**

For the potential (1) in (3.24) the natural choices for the range of integration with respect to a in expressions (2.2)-(2.3) are $\alpha_1 = 0$ and $\alpha_2 = 2^{1/6}d$. We start with the virial expansion of $g_2(n, a^+)$:

$$g_2(n,a^+) = 1 + \left(\frac{2\pi a^3}{3}\right)\frac{5}{8}n + \left(\frac{2\pi a^3}{3}\right)^2 b_4 n^2 + \left(\frac{2\pi a^3}{3}\right)^3 b_5 n^3 + \left(\frac{2\pi a^3}{3}\right)^4 b_6 n^4 + \cdots\,, \tag{4.1}$$

where b_k are the reduced virial coefficients for the hard-sphere system given by

$$B_1 = 1, \quad B_2 = \frac{2\pi a^3}{3}, \quad b_2 = 1, \quad b_3 = \frac{B_3}{B_2^2} = \frac{5}{8}, \tag{4.2}$$

$$b_4 = \frac{B_4}{\left(\frac{2\pi a^3}{3}\right)^3} = 89/280 + (219\sqrt{2}/2240\pi) + (4131/2240\pi)\cos^{-1}(1/\sqrt{3}) \approx 0.28695 \tag{4.3}$$

$$b_5 = \frac{B_5}{\left(\frac{2\pi a^3}{3}\right)^4} \approx 0.1102, \quad b_6 = \frac{B_6}{\left(\frac{2\pi a^3}{3}\right)^5} \approx 0.0386, \quad \ldots, \tag{4.4}$$

while B_k are the virial coefficients appearing in the hard-sphere equation of state:

$$\frac{p}{nk_BT} = 1 + \sum_{k=1}^{\infty} B_{k+1}n^k. \tag{4.5}$$

In terms of the (standard) reduced variables for the distance $r^* = r/d$, density $n^* = nd^3$, and the temperature $T^* = k_BT/\epsilon$, the equation of state (3.25) has the form

$$\begin{aligned}
\frac{p}{nk_BT} &= \\
1 &+ \left(\frac{2\pi d^3}{3}\right)\underbrace{\left(\int_0^{2^{\frac{1}{6}}} r^3P(r)\,dr\right)}_{v_2} n + \left(\frac{2\pi d^3}{3}\right)^2 \frac{5}{8}\underbrace{\left(\int_0^{2^{\frac{1}{6}}} r^6P(r)\,dr\right)}_{v_3} n^2 + \left(\frac{2\pi d^3}{3}\right)^3 b_4\underbrace{\left(\int_0^{2^{\frac{1}{6}}} r^9P(r)\,dr\right)}_{v_4} n^3 \\
&+ \left(\frac{2\pi d^3}{3}\right)^4 b_5\underbrace{\left(\int_0^{2^{\frac{1}{6}}} r^{12}P(r)\,dr\right)}_{v_5} n^4 + \left(\frac{2\pi d^3}{3}\right)^5 b_6\underbrace{\left(\int_0^{2^{\frac{1}{6}}} r^{15}P(r)\,dr\right)}_{v_6} n^5 + \cdots\,,
\end{aligned} \tag{4.6}$$

where, for simplicity of notation, we continue calling the reduced distance r^* by r and the density n^* by n. Our normalized $P(r)$ is taken from [1] (equation (2.26)). It corresponds to the repulsive part of the Lennard-Jones potential:

$$P(r) = \frac{\frac{d}{dr}\left[\exp(-\beta\phi^r(r)\right] Z(\beta\phi^r(r))}{\int\limits_0^{2^{1/6}} \left\{\frac{d}{dr}\left[\exp(-\beta\phi^r(r)\right] Z(\beta\phi^r(r))\right\}\,dr}, \tag{4.7}$$

where

$$Z(\beta\phi^r)(r) = \frac{\beta\phi^r(r)}{4}\exp\left(\frac{\beta\phi^r(r)}{2}\right)\left[K_1\left(\frac{\beta\phi^r(r)}{2}\right) + K_0\left(\frac{\beta\phi^r(r)}{2}\right)\right], \qquad (0 < r \le 2^{1/6}) \tag{4.8}$$

The functions $K_0(r)$ and $K_1(r)$ are the modified Bessel functions of order 0 and 1, respectively, and β is the inverse of reduced temperature. Equation (4.8) is derived by Leegwater from a consideration of two-particle dynamics using approximations that facilitate analytic representation.

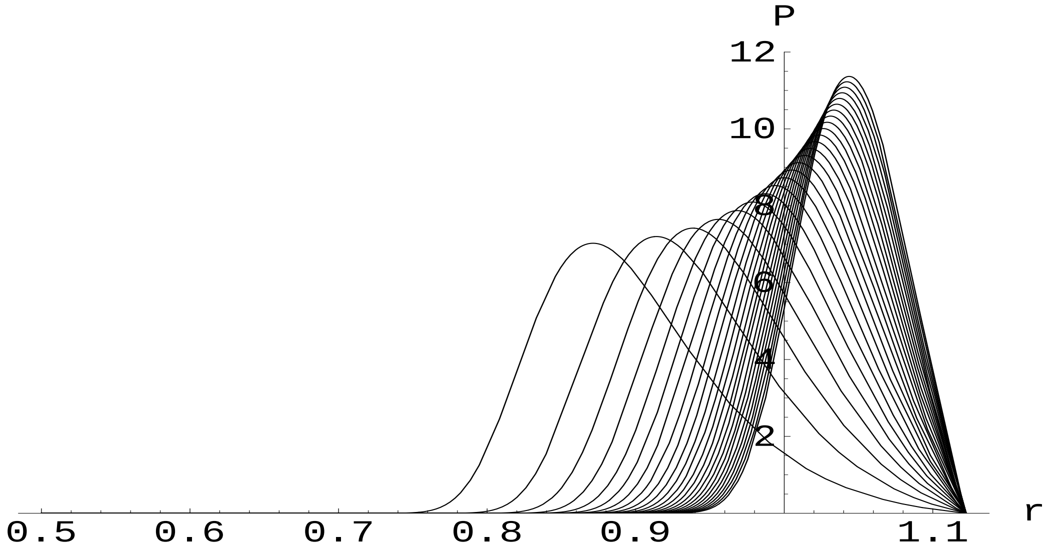

FIGURE 1. Graphs of $P(r)$ for $\beta = 0.1, 0.2, \ldots, 2.4, 2.5$. The leftmost graph corresponds to $\beta = 0.1$ and the rightmost graph corresponds to $\beta = 2.5$.

Next, we compare the reduced virial coefficients B_k^* for a system with the potential with ϕ^r (see (3.24)) with the virial coefficients given by our model in (4.6):

$$B_2^* \sim v_2, \quad B_3^* \sim \frac{5}{8} v_3, \quad B_4^* \sim b_4 v_4, \quad B_5^* \sim b_5 v_5, \quad \ldots \tag{4.9}$$

Due to space limitation we provide below only comparison of the second reduced virial coefficient B_2^*, given by

$$B_2^*(\beta) = \int_0^{2^{(1/6)}} [1 - \exp(-\beta\phi^r)]\, d(r^3), \qquad \text{(Here, } r^3 \text{ is the variable of integration.)} \tag{4.10}$$

with our v_2 (see (4.6)).

TABLE 1. The coefficient (see (4.6)) v_2 compared with B_2^* (see (4.10)) for different $\beta = 1/T^*$. The largest difference between v_2 and B_2^* is $< 8\%$. In the range of β between 0.25 and 2, the difference is $< 4\%$.

	$\beta = 0.25$	$\beta = 0.5$	$\beta = 0.75$	$\beta = 1$	$\beta = 1.25$	$\beta = 1.5$	$\beta = 1.75$	$\beta = 2$
v_2	0.857847	0.952418	1.00511	1.04069	1.06708	1.0878	1.1047	1.11886
B_2^*	0.879458	0.958876	1.00058	1.02722	1.04589	1.05971	1.07032	1.07866

	$\beta = 2.25$	$\beta = 2.5$	$\beta = 2.75$	$\beta = 3$	$\beta = 3.25$	$\beta = 3.5$	$\beta = 3.75$	$\beta = 4$
v_2	1.13098	1.14154	1.15084	1.15913	1.16659	1.17335	1.17953	1.18519
B_2^*	1.08536	1.09082	1.09532	1.09907	1.10222	1.10488	1.10714	1.10908

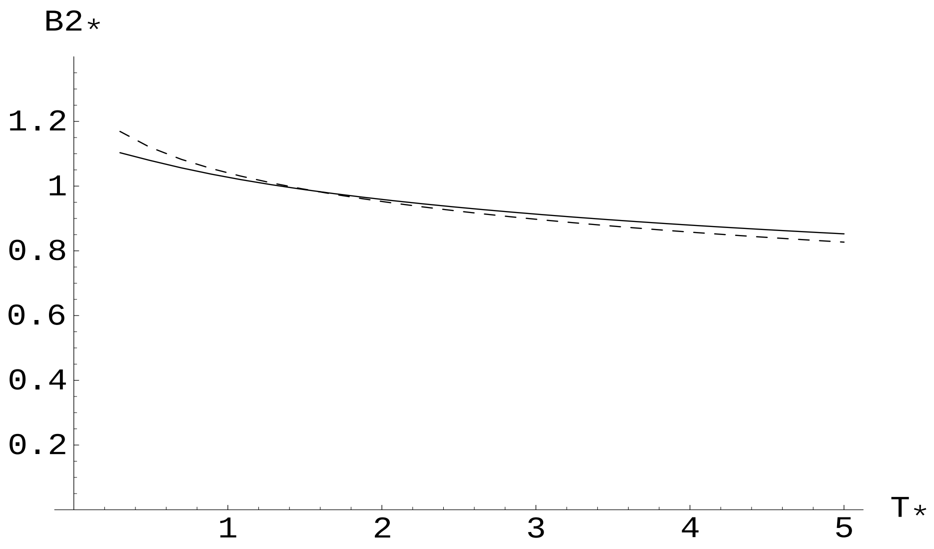

FIGURE 2. Graphs of v_2 (dashed curve) and B_2^* as functions of T^*.

For the potential ϕ^s (see (3.24)) with $\gamma = 1$ and $m = 12$, we compared the second ([19]) and third virial ([20]) coefficients of the system described by this potential with our v_2 and $b_3 v_3$. Using only numerical computations (with $\alpha_1 = 0$ and $\alpha_2 = \infty$), we found that

$$\frac{B_2^*}{v_2} = 1.11284 \qquad \text{and} \qquad \frac{B_3^*}{b_3 v_3} = 0.993476 \tag{4.11}$$

for all β. Furthermore, since the asymptotic behavior of the kth virial coefficient of the system described by the potential ϕ^s (with $\gamma = 1$) is given by $(\beta)^{3(k-1)/m}$ (see, [21], [22]), we checked numerically that the following relations are true

$$v_k(\beta, m) b_k = A(m,k) B_k^*(\beta, m) \qquad \text{for all } \beta > 0, \text{ all } k = 2,3,4,\ldots, \text{ and } m = 6, 9, 12, 15, 18. \tag{4.12}$$

In (4.12), $A(m,k) > 0$ is a computable function of m and k. In other words, the kinetic equation (2.1) with P given by (4.7), where ϕ^r is replaced by ϕ^s, correctly predicts temperature dependence of the system governed by the potential ϕ^s in its equation of state.

4.2. **Comparisons of the pressure.**

The expression for pressure (3.25) requires integration of the contact value $g_2(n, a^+)$ multiplied by $b^E(a)P(a)$ with respect to a. For numerical computations we considered two approximations of the hard-sphere $g_2(n, a^+)$:

$$g_2(n, a^+) \approx 1 + \sum_{k=1}^{8} \left(\frac{2\pi n a^3}{3}\right)^k b_{k+2} \tag{4.13}$$

and

$$g_2^{CS}(n, a^+) \approx \frac{3}{2\pi n a^3}\left[\frac{1 + \frac{\pi}{6} n a^3 + \frac{\pi^2}{36} n^2 a^6 - \frac{\pi^3}{216} n^3 a^9}{\left(1 - \frac{\pi}{6} n a^3\right)^3} - 1\right]. \tag{4.14}$$

The approximation in (4.13) is motivated by the fact that we know the hard-sphere reduced virial coefficient up to b_{10}. On the other hand, the expression in (4.14), is the well know Carnahan-Starling approximation ([23]) that is accurate over large values of the density n. For pressure comparisons, we consider only potential ϕ^r in the definition of $P(r)$.

Below, we present the graphs of the ratio of p/p_E as functions n^*, for the reduced temperatures $T^* = 0.5, 0.75, 1.0, 1.25, 1.5, 1.75, 2.0, 2.25, 2.5$, where p_E is the hard-sphere pressure given in (3.26), for both approximations of $g_2(n, a^+)$ in (4.13) and (4.14).

Overall, as expected, there are no significant differences in pressure except in the high-density region, where $n^* = na^3 \approx 0.9 - 1.2$.

Note: *The top graphs in Figures 3 and 4 correspond to* $T^* = 0.25$. *The lowest graphs in Figures 3 and 4 correspond to* $T^* = 2.50$.

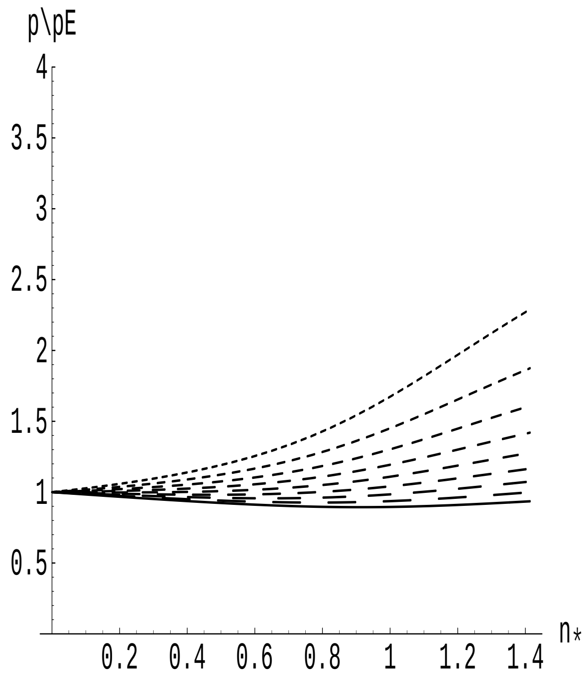

FIGURE 3. The ratio p/p_E as function of $n^* = nd^3$ for g_2 given by (4.13).

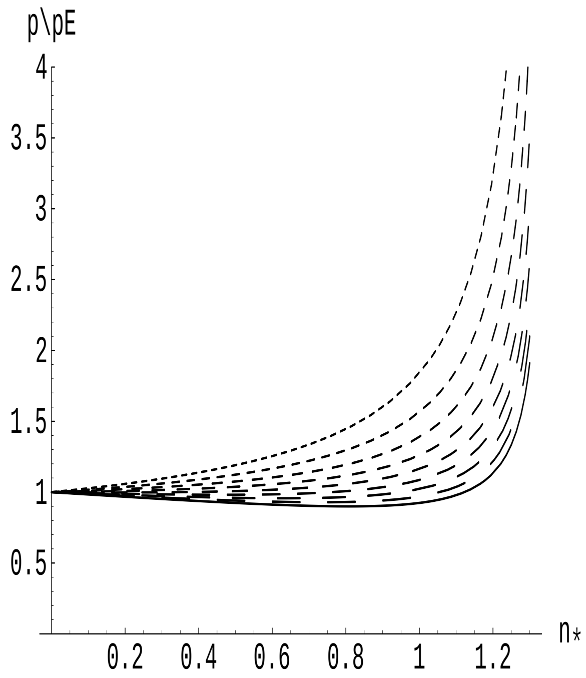

FIGURE 4. The ratio p/p_E as function of $n^* = nd^3$ for g_2 given by (4.14).

4.3. **Comparisons of the transport coefficients.**

As in the case of the pressure, we consider only potential ϕ^r in the definition of $P(r)$. We compared the ratios η^{stoch}/η^E, κ^{stoch}/κ^E, and D^{stoch}/D^E as the functions of the reduced density n^*, for various reduced temperatures $T^* = 0.5$, 0.75, 1.0, 1.25, 1.5, 1.75, 2.0, 2.25, and 2.5. Here η^E, κ^E, and D^E are the shear viscosity, the thermal conductivity, and the self-diffusion coefficients predicted by the (revised) Enskog equation.

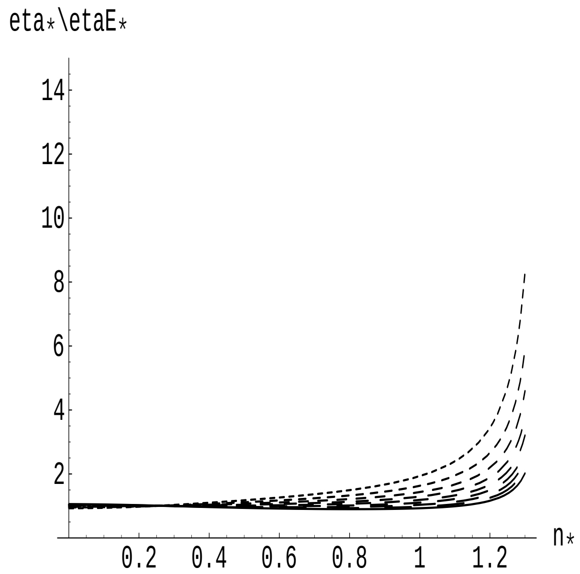

FIGURE 5. The ratio η^{stoch}/η^{E} as function of $n^* = nd^3$ for g_2 given by (4.14).

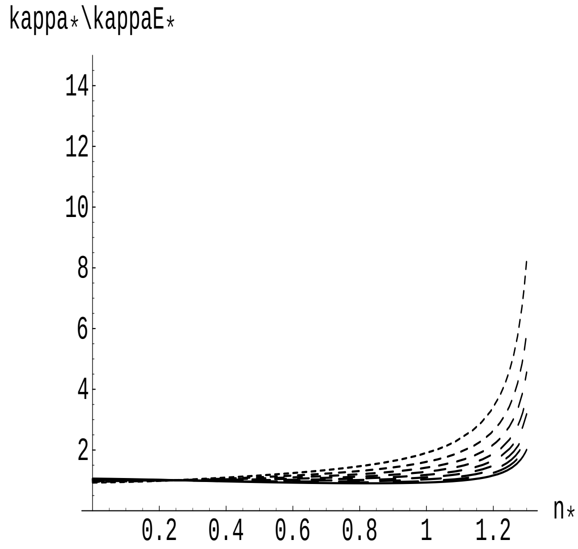

FIGURE 6. The ratio $\kappa^{stoch}/\kappa^{E}$ as function of $n^* = nd^3$ for g_2 given by (4.14).

Note: *The top graphs in Figures 5 and 6 correspond to $T^* = 0.25$. The lowest graphs in Figures 5 and 6 correspond to $T^* = 2.50$.*

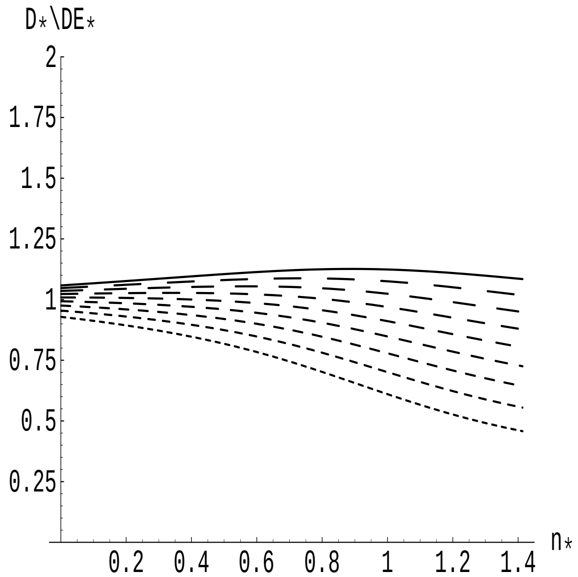

FIGURE 7. The ratio D^{stoch*}/D^*_E as a function of $n^* = nd^3$ and T^* for g_2 given by (4.13).

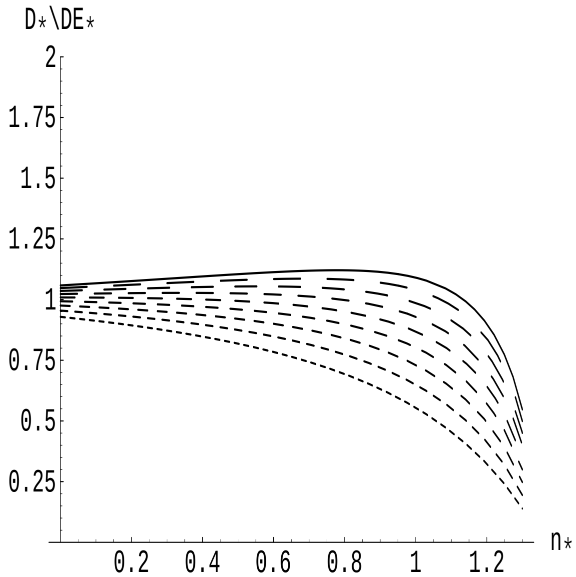

FIGURE 8. The ratio D^{stoch*}/D^*_E as a function of $n^* = nd^3$ and T^3 for g_2 given by (4.14).

Note: *The top graphs in Figures 7 and 8 correspond to $T^* = 2.5$. The lowest graphs in the Figures 7 and 8 correspond to $T^* = 0.25$.*

Finally, Table 2 provides absolute values of the η^{stoch}, κ^{stoch}, and D^{stoch} for various densities $n^* = nd^3$ with $d = 3.405 \times 10^{-10}$ m, mass=39.95 au, and various reduced temperatures $T^* = k_B T/\epsilon$ in Lennard-Jones units and $\epsilon/k_B = 119.8$ K. Our results are given for the approximation of $g_2(n, a^+)$ in (4.13) and for the Carnahan-Starling approximation (4.14) (with the (CS) marking).

TABLE 2. Comparison of the transport coefficients from our model and experiments. Numbers in the brackets, in the fourth column of the table, are the references from the work of Karkheck, Stell, and Xu ([11]) that indicate the sources of the corresponding experimental or computer simulation data.

State	Transport coefficient	Our values	Simulation (S) Experiment (E)
Liquid (triple point) $n^* = 0.844,\ T^* = 0.73$	η (in $\mathrm{Pa\,s} \times 10^{-4}$)	3.75 3.81 (CS)	2.62–2.89 (S) [12−17] 2.71 (E) [18, 19] 2.76 (E) [20]
Liquid (triple point) $n^* = 0.844,\ T^* = 0.73$	κ (in $\mathrm{mJ\,K^{-1}\,m^{-1}\,s^{-1}}$	198 202 (CS)	127 (S) [21, 22] 134 (S) [17] 133 (E) (±4%) [23]
Liquid $n^* = 0.818,\ T^* = 0.761$	D (in $\mathrm{cm^2\,s^{-1}} \times 10^{-5}$)	1.89 1.83 (CS)	2.30 (S) [24]
Liquid $n^* = 0.715,\ T^* = 0.94$	κ (in $\mathrm{mJ\,K^{-1}\,m^{-1}\,s^{-1}}$	114 114.5 (CS)	94 (S) (±5%) [21] 90 (E) (±4%) [23]
Supercritical $n^* = 0.20,\ T^* = 1.60$	η (in $\mathrm{Pa\,s} \times 10^{-4}$)	0.228 0.228 (CS)	0.226 (E) [23]
Dense hot supercritical $n^* = 1.040,\ T^* = 2.51$	η (in $\mathrm{Pa\,s} \times 10^{-4}$)	4.66 4.89 (CS)	4.85 (S) [13] 5.78 (S) [14] 4.80 (E) [25]
Dense hot supercritical $n^* = 1.074,\ T^* = 2.502$	D (in $\mathrm{cm^2\,s^{-1}} \times 10^{-5}$)	3.55 3.11 (CS)	3.10 (S) [24]

4.4. **Concluding remarks.**

We are proposing the use of our stochastic modeling to extend the revised Enskog theory and the KVTIII in a new way to apply to softened continuous potentials, such as the RLJ and LJ potentials. We clearly can not expect the results to be any better for such potentials than the underlying RET or KVTIII results already are for hard-sphere and square-well potentials. In particular, we can not hope to capture backflow and caging effects that are important at liquid-state densities, but are left out of the RET and KVTIII. To capture these effects, we propose tagging a particle and assigning an effective diameter and reduced mass in its interaction with other particles according to the prescriptions developed by Sung and Stell [24]. Unlike Sung and Stell, however, we intend to use those prescriptions in the context of the KVTIII, with our stochastic modeling enabling us to extend our results to soft-core continuous potentials.

References

[1] J. A. Leegwater, *Kinetic theory of dense fluids*, Ph. D. Dissertation, University of Utrecht, 1991.

[2] *Kinetische Theorie*, Kgl. Svenska Vetenskaps Akademiens Handl **63**, no. 4 (1921) [English translation in S. Brush, **Kinetic Theory**, Vol. 3 Pergamon Press, New York, 1972.

[3] H. van Beijeren and M. H.Ernst, *The modified Enskog equation*, Physica **68** (1973), 437-456.

[4] P. Résibois and M. DE. Leener, **Classical Kinetic Theory of Fluids**, John Wiley & Sons, New York, 1977.

[5] H. T. Davis, Stuart A. Rice, and J. V. Sengers, *On the Kinetic Theory of Dense Fluids. IX. The fluid of Rigid Spheres with a Square-Well Attraction*, J. Chem. Phys. **35** (1961), 2210-2233.

[6] J. Karkheck, G. Stell, *Maximization of entropy, kinetic equations, and irreversible thermodynamics*, Phys. Rev. A **25** (1982), 3302–3327.

[7] G. Stell, J. Karkheck, and H. van Beijeren, *Kinetic mean field theories: Results of energy constraint in maximizing entropy*, J. Chem. Phys. **79** (1983), 3166–3167.

[8] J. Karkheck, H. van Beijeren, I. de Schepper, and G. Stell, *Kinetic theory and H theorem for a dense square-well fluid*, Phys. Rev. A **32** (1985), 2517–2520.

[9] J. Bławzdziewicz and G. Stell, *Local H-theorem for a kinetic variational theory*, J. Stat. Phys. **56** (1989), 821–840.

[10] H. van Beijeren, *Kinetic theory of dense gases and liquids*, in **Fundamental Problems in Statistical Mechanics VII**, H. van Beijren Ed., Elsevier (1990), 357-380.

[11] J. Karkheck, G. Stell, and J. Xu, *Transport theory for the Lenard–Jones dense fluid*, J. Chem. Phys. **89** (1988), 5829–5833.

[12] A. Ya. Povzner, *The Boltzmann equation in the kinetic theory of gases*, Amer. Math. Soc. Transl. **ser. 2, 47** (1962), 193–216.

[13] M. Lachowicz and M. Pulvirenti, *A stochastic system of particles modeling the Euler equation*, Arch. Rat. Mech. Anal., **109** (1990) 81–93.

[14] M. Pulvirenti, *Kinetic limits for stochastic Particle Systems*, in **Lecture Notes in Mathematics** D. Talay and L. Tubaro, editors, Springer Verlag **1627**, 1995, 96–126.

[15] N. Bellomo and J. Polewczak, *The generalized Boltzmann equation existence and exponential trend to equilibrium*, C. R. Acad. Sci. Paris **319**, Série I, (1994), 893-898.

[16] D. Ruelle, **Statistical mechanics**, Benjamin, London, 1969.

[17] J. Polewczak and G. Stell, *New properties of a class of generalized kinetic equations*, J. Stat. Phys. **64** (1991), 437–464.

[18] M. Mareschal, J. Bławzdziewicz, and J. Piasecki, *Local entropy production from the revised Enskog equation: General formulation for inhomogeneous fluids*, Phys. Rev. Lett. **52** (1984), 1169–1172.

[19] J. Jeans, **Dynamical Theory of Gases**, Cambridge University Press, Cambridge, 1925.

[20] T. Kihara and T. Hikita, in **Fourth Symposium on Combustion**, Williams and Wilkins Co., Baltimore, 1953, 458.

[21] J. S. Rowlinson, *An equation of state of gases at high temperatures and densities*, Molecular Phys. **7** (1964), 349.

[22] J. S. Rowlinson, *The statistical mechanics of systems with steep intermolecular potentials*, Molecular Phys. **8** (1964), 107.

[23] N. F. Carnahan and K. E. Starling, J. Chem. Phys. **51** (1969), 635.

[24] W. Sung and G. Stell, J. Chem. Phys. **80** (1984), 3350.

Department of Mathematics, California State University, Northridge, CA 91330-8313

E-mail address: `jacek.polewczak@csun.edu`

Department of Chemistry, State University of New York at Stony Brook, Stony Brook, NY 11794-3400

E-mail address: `gstell@mail.chem.sunysb.edu`